International Journal of Science and Research (IJSR)
ISSN: 2319-7064
ResearchGate Impact Factor (2018): 0.28 | SJIF (2018): 7.426

Second Harmonic Generation of 236.5 nm Laser Beam by BBO Crystal Using Comsol Software

Raneen Salam Al-Obaidi[1], Suha Mousa Alawsi[2]

[1]Al-Nahrain University, College of Science, Department of Physics, Baghdad, Iraq

Abstract: ***Comsol of version 5.3a is used to design and simulate the SHG. The available tools in this software enable to introduce the best boundary conditions that suitable in the use with the nonlinear material of SHG. The simulation of SHG is carried out by two ways, they are: frequency domain and temporal domain. Both are employed to achieve double the frequency of the considered laser sources; blue laser of 473nm wavelength, and using BBO crystal of optical path 3×3×5mm. In fact, the results of temporal transform based Comsol showed the ability to implement the SHG experiment and achieving the double frequency (1.268 x$10^{15}s^{-1}$) of wavelength of 236.5nm laser besides the fundamental frequency (0.634x$10^{15}s^{-1}$) of 473nm wavelength laser. While the frequency domain results showed that the obtained photon flux density 2.4x10^{25} Photon/m^2s for the laser of wavelength of 473nm at the point of meeting the fundamental and second harmonic photon flux density***

Keywords: nonlinear optics, second harmonic generation, Comosl programming

1. Introduction

Nonlinear optics is an important field in physics due to its occupation a wide extreme range of recent applications that related to the propagation of electromagnetic waves. It is based on studying the interaction of high intensity light with matter while its propagation [1]. One of the most important physical phenomena in the nonlinear optics is the second harmonic (SH), which is a useful tool to change the wavelength of the laser beam from one value to another. A high-intensity light source is needed to generate SH, which can be achieved only by using lasers [2]. Nonlinear optics is practically employed to change the wavelength of the laser to achieve increased advantages of these rays, and can be through this technique to obtain wavelengths longer or shorter than the wavelength of the laser pump. This technique leads to save the time, effort, and price in manufacturing of laser devices of desired wavelength. Such that, the second harmonic generation (SHG) became an important part of nonlinear optics and has opened up new fields and continuous researches to obtain the highest conversion rate, and maximum possible energy at the new required wavelength of coherent light [3]. Jeremiah Birrell in 2007 determined the optimal parameters for maximizing SHG of 423*nm* light for use in an atom interferometer. The analysis is done using the nonlinear crystal Beta BBO, where both critical and noncritical phase matching methods are considered [4]. Antonczak A.J. et al in 2010 presented a built in design of diode-pumped CW of Nd:YAG low power laser that operates at 946*nm* to interact blue light of 473*nm* that useful for applications of battery operation. The used nonlinear crystal is a BiBO crystal cutting at phase-matching of I-type. In this experiment, the used pumping power 20*mW* gave stabile output power of 0.8*W* of blue light. The conversion efficiency of SHG was about 2.5% [5]. Bache M. et al in 2013 studied the response of isotropic nature of beta-mode of the nonlinear crystal BBO. The study focuses on the determination of the components of cubic tensor $X^{(3)}$ that affecting the SHG interaction of I-type, the discussion impact the subject of usage the response of cubic anisotropic in BBO based cascaded ultrafast experiments [6]. Takashi Sekine in 2013 demonstrated the SHG of 12.5*J* was giving a conversion efficiency of 71.5% at 0.6*Hz* repeating rate from a laser of Nd:glass diode-pumped. The system consists of nonlinear crystal CLBO for doubling the frequency. The results indicate the highest output characteristic of energy and respect conversion efficiency by SHG of diode-pumped laser from a CLBO were achieved [7]. Masada G. in 2014 showed the efficient generation of second harmonic waves of 200*mW* with 70% of conversion efficiency at 473*nm* was achieved by using a periodically poled $KTiOPO_4$ crystal inside an external cavity. The calculation based on the theory of SHG with an external resonator show good agreement with the experimental results [8]. Jianhua Zeng in 2019 determined the location of the waist of Gaussian spreading beam depending on symmetry changes of SHG intensity at two sides of waist for monolayer MoS2 on substrate SiO2/Si. The radius of waist is beneficially computed, which was leading to determine the research optical property of MoS2 and further some electromagnetic materials [9].

2. SHG Theory

The proposed SHG model is based on the laser-material interaction that generating SHG in nonlinear crystal. This depends on introducing an interaction between laser beam and nonlinear crystal which leads to an expected reaction impact the wavelength of the incident laser. When the laser beam incident on the nonlinear crystal, the frequency of the laser beam is duplicated, implies obtaining a new shorter laser wavelength, and so on one can choose the laser source and proper nonlinear crystal to achieve the intended short wavelength laser. Comsol of version 5.3a is used for designing and simulating the SHG. The tools available in Comsol software give the ability of introducing desired boundary conditions that are properly useful with nonlinearity based SHG. This work includes two ways to implements the SHG experiment, they are: frequency domain and temporal domain. Both are employed to achieve half the wavelength of a laser source; blue laser of 473*nm* wavelength, and using BBO crystal of optical path 3×3×5*mm*.

			generation

3. SHG Design by Comsol

The design of SHG experiment is carried out using Comsol Multiphysics simulation software of version 5.3a.

Boundary Conditions of Temporal Transformation

This model shows how setup the SHG as a transient wave simulation using nonlinear material properties. The laser of DPSS type ($\lambda = 0.473\mu m$) is focused on a nonlinear crystal, so that the waist of the beam is positioned inside the crystal. To simplify the problem and reduce the calculation time, this model is adopted with no full 3D simulation, but rather a 2D model. The model uses Comsol Multiphysics' standard 2D coordinate system. The propagated the laser beam behaved like approximated plane wave of Gaussian distributing the intensity cross section. At focal point, the beam of laser has its minimum width of ω_o. The time based solution of Maxwell's equations for a 2D geometry gives the following electric field [10]:

$$E_{(x,y,z)}=E_o\sqrt{\frac{\omega_o}{\omega(x)}}e^{-(y/\omega(x))^2}\cos\left(\omega t-kx+\eta(x)-\frac{ky^2}{2R(x)}\right)e_z \quad (1)$$

Where:

$$\omega(x) = \omega_o\sqrt{1+\left(\frac{x}{x_o}\right)^2} \quad (2)$$

$$\eta(x) = \frac{1}{2}\operatorname{atan}\left(\frac{x}{x_o}\right) \quad (3)$$

$$R(x) = x\left(1+\left(\frac{x_o}{x}\right)^2\right) \quad (4)$$

In these expressions, ω is angular frequency, ω_o is minimum waist, *k* is wave number, and *y* is transverse coordinate of in-plane. The beam wave-front isn't planar exact, it is propagating as spherical wave of radius $R(x)$. Almost, the wave is seems to be plane close the focal point. The laser beam is also modeled as a time pulse in terms of enveloped Gaussian function. This is producing a package of waves of spectrum is frequency Gaussian distribution. These expressions are used as the input boundary conditions. And the input parameters for ($\lambda = 473nm$) are listed in the Table (1):

Table 1: Entered parameters of 473*nm* laser in Comsol software using temporal transformation

Name	Expression	Value	Description
ω_o	564 [um]	5.64E-4 m	Minimum spot radius of laser beam
Lambda	0.473[um]	4.73E-7 m	Wavelength of input laser beam
E_o	30[KV/m]	30000 V/m	Peak electric field
x_o	Pi*ω_o^2/lambda	1.8784 m	Rayleigh range
k_o	2*pi/lambda	1.181E7 1/m	Propagation constant
Omega	k_o * c_const	3.5407E15 1/s	Angular frequency
t_o	25[fs]	2.5E-14 s	Pulse time delay
dt	10[fs]	1E-14 s	Pulse width
d_{33}	1.341e-17[F/V]	1.341E-17 $s^7.A^3/(kg^2.m^4)$	Matrix element for second harmonic

Boundary Conditions of Frequency Domain

The frequency based model demonstrates how two frequency-domain interfaces can be coupled together to simulate the process of SHG. Where, light from the fundamental wavelength (or, frequency) is injected in a nonlinear crystal that generates the second harmonic frequency, which is twice the fundamental frequency. The results are compared with analytical results obtained within the Slowly Varying Envelope Approximation (The slow variation of enveloped approximation (SVEA) to calculate and model the propagation of light is employed for simplifying scalar form of Maxwell's equations, which are describing the electromagnetic waves propagation in vacuum or material. SVEA operated correctly in propagation angles of narrow range). Such model geometry is simple, it consist of a slender two-dimensional rectangle. The rectangle is many wavelengths long in the propagation direction, but consists of only one mesh element in direction is orthogonal to the propagation direction. The first Electromagnetic Waves, Frequency Domain interface is defined for the fundamental frequency f1 and the second Electromagnetic Waves, Frequency Domain interface is defined for the second harmonic frequency 2f1. The only incident wave is polarized in the y-direction and launched at the fundamental frequency using a Scattering Boundary Condition feature. The two interfaces are coupled using a Polarization feature added to each of the interfaces. For the fundamental interface, the polarization is given by

$$P_{1y} = 2dE_{2y}E_{1y}^* \quad (5)$$

While the polarization for the second harmonic interface is given by:

$$P_{2y}=d\,E_{1y}^2 \quad (6)$$

Where d is a nonlinear coefficient for the process, $E1y$ is the y-component of the electric field at the fundamental frequency, and $E2y$ is the y-component of the electric field at the second harmonic frequency. The results from the simulation are compared with the analytical results obtained within the Slowly Varying Envelope Approximation (SVEA). The analytical results for the photon flux density with assumption of perfect phase matching, are computed by the following formula for the fundamental wave:

$$\varphi_1(x) = \varphi_1(0)\,\mathrm{sech}^2\left(\frac{\gamma x}{2}\right) \quad (7)$$

and it is computed using the following formula for the second harmonic wave:

$$\varphi_2(x) = \frac{1}{2}\varphi_1(0)\tanh^2\left(\frac{\gamma x}{2}\right) \quad (8)$$

Where $\varphi 1(0)$ is the incident photon flux density for the fundamental wave, in which the constant ϒ is defined as follows:

$$\gamma = 8d^2Z_0^3\omega^2 I_1(0) \quad (9)$$

where, Zo is the characteristic impedance of the medium, ω is the angular frequency, and I1(0) is the incident intensity for the fundamental wave. As given in Equations (1.7 and 1.8), when x goes to infinity the photon flux density for the fundamental goes to zero, whereas the photon flux density for the second harmonic approaches half of the initial fundamental photon flux density. Since the photon energy for the second harmonic is twice that of the fundamental, the energy is conserved in the process. The input parameters for (λ = 473nm) are shown in following Table (2).

Table 2: Entered parameters of 473nm laser in Comsol software using Frequency Domain

Name	Expression	Value	Description
Lambda 1	0.473 [um]	4.73E-7 m	Fundamental wavelength
f1	c_const/lambda 1	6.3381E14 1/s	Fundamental frequency
f2	2*f1	1.2676E15 1/s	Second harmonic frequency
Lambda 2	c_const/f2	2.365E-7 m	Second harmonic wavelength
Sim_I	Lambda 1*25	1.1825E-5 m	Simulation length
Sim_h	Lambda 2/16	1.4781E-8 m	Simulation height
d	1.341e-18[C/V^2]	1.341E-18 $s^7.A^3/(kg^2.m^4)$	Nonlinear coefficient
L	Sim_I-3*lambda 1	1.0406E-5 m	Length of nonlinear region
I1	30[MW/m^2]	3E7 W/m^2	Incident fundamental intensity
E1	Sqrt(2*I1/c_const/epsilon0_const)	1.5035E5 V/m	Incident fundamental electric field strength
Offset	1.5*lambda 1	7.095E-7 m	Start of nonlinear region

4. Result and Discussion

1) Temporal Transformation

The simulation of the temporal transformation indicates the effect of the SHG on the laser beam of wavelength 473nm when the laser beam travels along the simulated design of proposed experiment setup. When the laser beam is propagating through the crystal in the direction of the x-axis, it has a transverse Gaussian beam is in the direction of the y-axis. The Gaussian beam is monochromatic electromagnetic radiation. And since the electric field is much more than the magnetic field, so the magnetic field is neglected. And that the electric field is polarized in the out of z-direction. And the intensity of the electric field depends on the intensity of the laser, the greater intensity of the laser increased the number of photons that generated the electric field, and then leads to increasing the intensity of the electric field. Figures (1-5) show the surface electric field of the laser of λ = 473nm at different characteristic time measured in femtosecond, while Figure (6) shows electric field intensity versus frequency for 473nm laser.

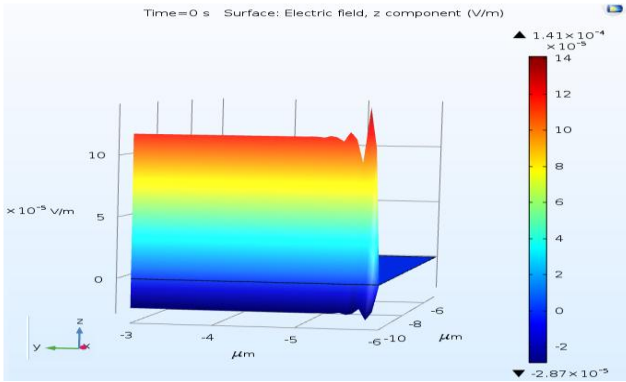

Figure 1: Electric Field intensity of 473*nm* laser inside the crystal by Comsol at time=0*fs* using temporal domain

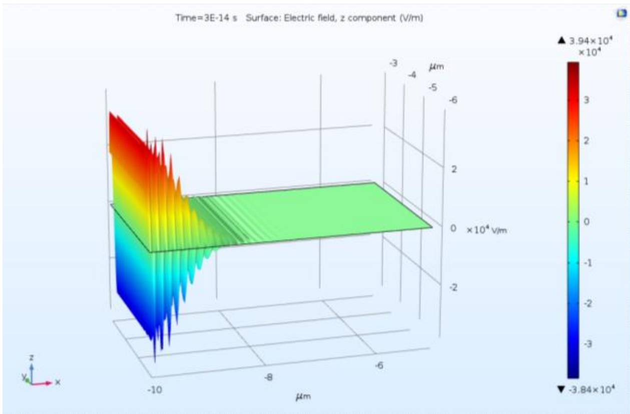

Figure 2: Electric Field intensity of 473*nm* laser inside the crystal by Comsol at time=30*fs* using temporal domain

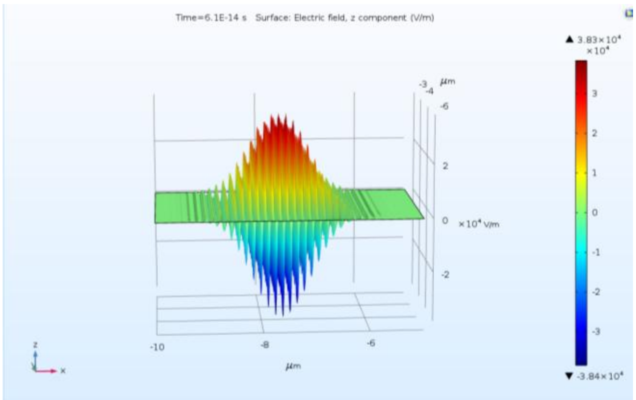

Figure 3: Electric Field intensity of 473*nm* laser inside the crystal by Comsol at time=61*fs* using temporal domain.

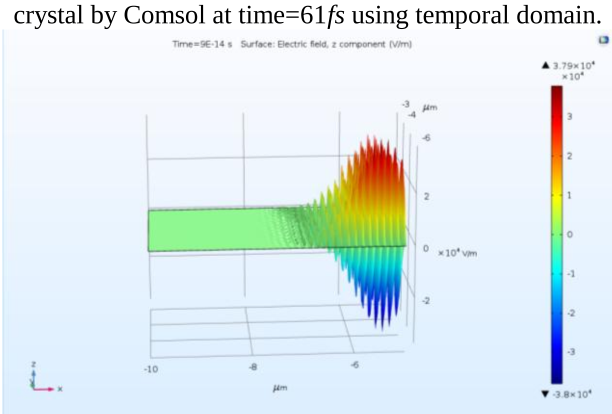

Figure 4: Electric Field intensity of 473*nm* laser inside the crystal by Comsol at time=90*fs* using temporal domain.

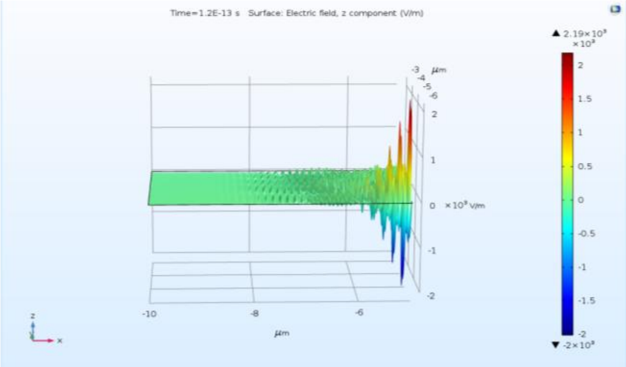

Figure 5: Electric Field intensity of 473*nm* laser inside the crystal by Comsol at time=120*fs* using temporal domain.

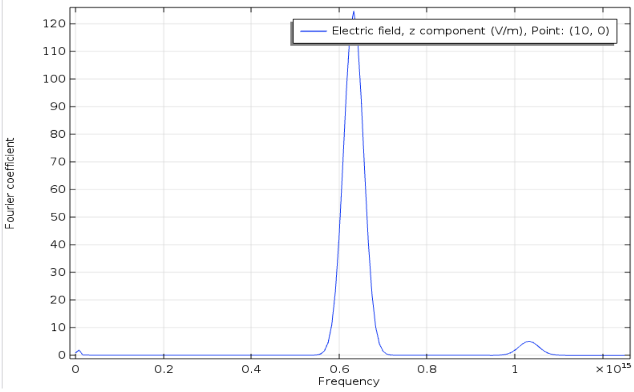

Figure 6: Electric Field intensity versus frequency for 473*nm* laser using temporal domain.

It is noticeable that the electric field intensity shown in Figure (3) indicates that the pulse had reached the output boundary after 61fs. While the pulse is completely disappeared after 120fs as shown in Figure (5). The simulation stores the time between 60fs and 120fs, which is when the pulse passes the output boundary. The electric field at this boundary has a second harmonic component that can be extracted using a frequency analysis. Also, it is shown that the electric field intensity given in Figure (1) is very little at zero time and about 1.41×10^{-4}v/m, which is reasonable result at the start edge of the crystal. After 30fs, the intensity of the electric field raised up to its maximum to be 3.94×10^{4}v/m, and then decay gradually to be at minimum value of about 2.19×10^{4}v/m after 120fs.

Results analysis showed that the intensity of the electric field became higher with reducing the time duration of the laser pulse. While the overall outcome system is measured depending on its ability to product a number of photons, the maximum power of pulse laser system is occurred when a number of photons are found in a pulse of less width and higher amplitude. Figure (6) shows that the frequency spectrum of the beam at the output boundary. The small peak on the right side of the large peak is the second harmonic generation and it is equal to $1.268 \times 1015 S^{-1}$. The smaller peak close to zero frequency is due to difference frequency generation. Thus, the fundamental frequency is appeared in Figure (6) at 473nm wavelength (ω=$0.643 \times 10^{15} S^{-1}$), while the SHG peak appear at a position after the fundamental one in a wavelength of 236.5nm (2ω =$1.286 \times 10^{15} S^{-1}$), which is ensure the duplication happen in the frequency of the used laser.

2) Frequency Domain

Frequency domain is another phase that adopted to simulate the proposed SHG experiment design. Comsol software prepare a specific tool to show the results of laser beam behavior in terms of frequency domain throughout its propagation into detector side. Figure (7) shows the resulted y-component of the electric field of the fundamental laser beam. It is shown that the amplitude decreases with propagating the laser in the medium, which also pictures the way of transferring the energy into the second harmonic wave. In addition, Figure (8) shows the y-component of the electric field for the second harmonic wave. For this wave, the initial amplitude is zero. Upon propagation, the amplitude increases while the energy transferred from the fundamental beam into SHG beam. It noticed the wavelength of second harmony field equal half the fundamental one. Also, Figure (9) shows a comparison between the y-components of the electric fields of the fundamental and the second harmonic one for the considered 473nm laser beam.

Furthermore, Figure (10) shows the photon flux density (in units of photons per m^2 and s) of second harmonic wave beside the fundamental one. The diamonds represent simulated results (green diamonds representing the second harmonic wave and blue diamond representing the fundamental wave), whereas the red line represents the analytical result of Equation (7) and the cyan line represents the analytical results of Equation (8). These behaviors shown in Figure (10) indicate a comparable simulated result with the analytical results obtain by applying the Slowly Varying Envelope Approximation (SVEA). This result state that the energy of each photon in the wave of second harmony is twice its amount of the photons in the fundamental wave. The curves indicate that the energy is conserved in the process of SHG.

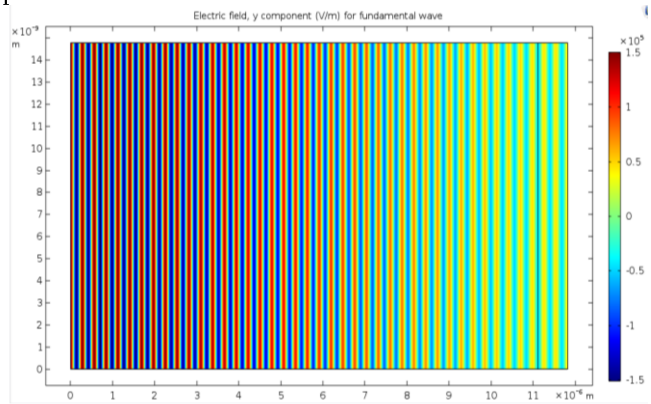

Figure 7: Intensity of electric field of 473*nm* laser inside the crystal by Comsol using frequency domain

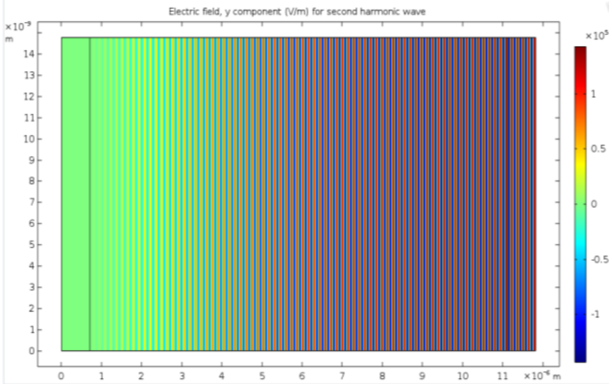

Figure 8: Electric Field intensity of 473*nm* laser inside the crystal by Comsol using frequency domain

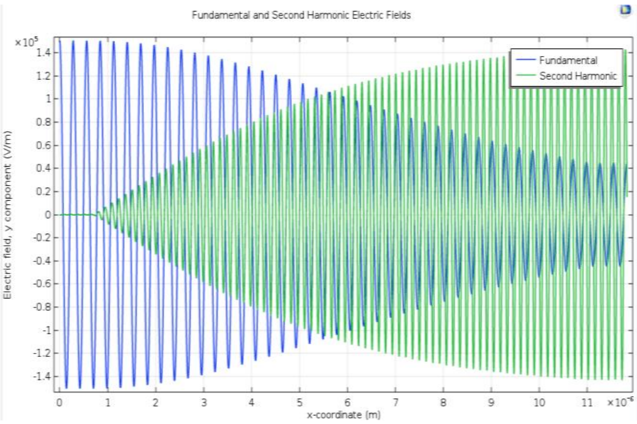

Figure 9: Comparison of Y-component of electric field intensity of 473nm laser for fundamental and second harmonic pulses

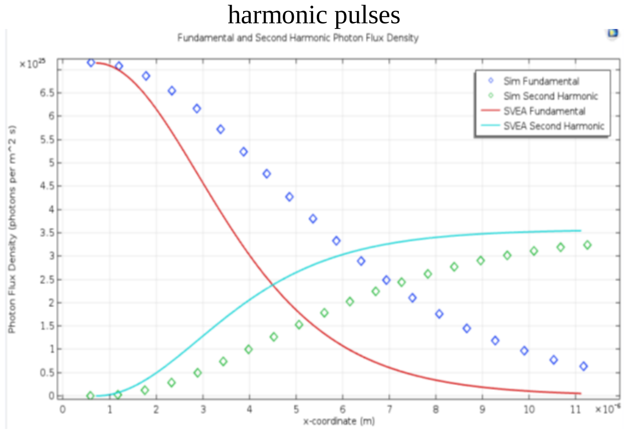

Figure 10: Photon density inside the crystal by Comsol for 473nm laser using frequency domain

In Figure (10) the behavior of the simulated fundamental laser beam is increasing gradually with its propegation along x-axis. Then, its behavior became curved with less increasing at each distance toward the boundary of crystal. While, the secondary harmonic pulse begins with a larger value and then decay toward zero at the boundary. Both fundamental and secondary harmonic behaviors intersect at one point of convergence at $6.8\times10^{-6}m$ position in x-axis. At this point, the number of photons that indicates the flux intensity are same and equal to 2.4×10^{25} $photons/m^2.s$ for the wavelength 473*nm*

References

[1] Boyd, R. (2007). "The Nonlinear Optical Susceptibility". Nonlinear optics (third edition). p. 2. doi:10.1016/B978-0-12-369470-6.00001-0
[2] O. Zvelto "Principles of Lasers" 2end Edition, translated by Dr.Manam M.(1988).
[3] K.D. Singer,and Y. Wu, "16-Second harmonic generation (SHG) as a characterization technique and phenomological probe for organic materials," Woodhead Publishing Limited, 2013, Pages 442-469.
[4] Jeremiah Birrell, "DESIGN OF A FREQUENCY-DOUBLED 423 nm LASER FOR USE IN A CALCIUM INTERFEROMETER," Brigham Young University, 2007.
[5] Arkadiusz J. Antonczak, Jaroslaw Sotor, Mateusz Matysiak, and Krzysztof M. Abramski, "Blue 473-nm solid state diode pumped Nd:YAG/BiBO microchip laser," OPTO−ELECTRONICS REVIEW, Rev., 18, no. 1, 2010.
[6] Morten Bache, Hairun Guo, Binbin Zhou, and Xianglong Zeng, "The anisotropic Kerr nonlinear refractive index of the beta-barium borate (b -BaB2O4) nonlinear crystal," Optical Society of America, 2013.
[7] Takashi Sekine, Hiroshi Sakai, Yasuki Takeuchi, Yuma Hatano, Toshiyuki Kawashima, Hirofumi Kan, Junji Kawanaka, Noriaki Miyanaga, and Takayoshi Norimatsu, "High efficiency 12.5 J second-harmonic generation from CsLiB6O10 nonlinear crystal by diode-pumped Nd:glass laser," Optical Society of America, vol. 21, No. 7, 2013.
[8] Genta Masada, "Efficient Generation of Second Harmonic Wave with Periodically Poled KTiOPO4 crystal at 473 nm," Tamagawa University Quantum ICT, Vol.4 No.1, 2014.
[9] Jianhua Zeng, Shanyu Du, Zhiwen Sang, Shan Chang, Penghao He, and Qiu Tu, "Determination of the waist location for the Gaussian beam based on second harmonic generation of monolayer MoS2," Material Science and Engineering, 2019.
[10] A. Yariv, Quantum Electronics, 3rd Edition, John Wiley & Sons, 1988.

Author Profile

Raneen Salam received the B.S. degrees in Physics from Al-Nahrain University in ,2014. During 2010-2014, i stayed in Advanced Photonics Laboratory to modify and improve performance of optical systems.

Suha M. Khorsheed received the B.S., M.S., and Ph.D. degrees in Physics from Al-Nahrain University in 1995,2000, and 2007, respectively. During 2007-2016, she stayed in Advanced Photonics Laboratory to modify and improve performance of optical systems. She now lecturer in the Physics Department- College of Science in Al-Nahrain University.